

CAPILLARY ABSORPTION OF HEAT PIPE WICKS

M. G. Semena, A. G. Kostornov,
A. N. Gershuni, A. L. Moroz,
and V. K. Zaripov

UDC 536.248.2

The capillary absorption kinetics in metal-fiber wicks for low-temperature heat pipes is investigated. The experimental results agree with the preliminary conclusions concerning optimum wick structures.

The growing interest in the development and investigation of heat pipes is due to the possibility of utilizing them successfully in various branches of modern technology. The most important structural element of a heat pipe is the wick, in which a liquid heat-transfer agent moves under the action of the capillary potential.

The limited heat-transfer capacity, which is a result of the transport properties of wicks, is one of the basic factors in the operation of low-temperature heat pipes. The transport properties of a wick, determined by the characteristics of the porous material (porosity, pore distribution, mean pore diameter, and permeability), are estimated, in the final analysis, with respect to the flow rate and the maximum rise height of the operating liquid. The flow rate and the rise height are also affected by the wetting contact angle. However, this parameter depends only on the surface phenomena at the wick-liquid interface.

Although the structural and hydrodynamic characteristics of porous wick materials have been investigated in many papers, few of them are devoted to experimental investigations of the capillary absorption rate [1-3]. These investigations were not concerned with optimum porous structures. Glass fabric was used as the wick material in [1, 2], and Refrazil (material based on silicon dioxide fibers) was used in [3]. However, in most cases, it is advisable to use metal wicks (gauze, powder, or fibrous materials) in heat pipes.

We provide here the results of an experimental investigation of the characteristics of capillary absorption by wick specimens made of high-porosity fibrous copper materials.

An investigation of the structural and hydrodynamic characteristics of materials with different ratios of the length of initial, monodisperse discrete fibers to their diameter ($l_f/d_f = 45, 75, 150$) was carried out before the experiments described here were performed. In particular, dependences of the permeability factor K , the mean pore diameter D_{me} , and the capillary pump parameter K/D_{me} on the porosity Π were determined for the range $\Pi = 58-96\%$. The relationships obtained led to preliminary conclusions concerning optimum porous structures, which are the following:

1. Wicks with a maximum value of K/D_{me} are best for heat pipes operating in the horizontal position.
2. Wicks operating against the force of gravity should be optimized first with respect to the mean pore diameter, which determines the required height of capillary rise. Then from the obtained structure variants with the same mean pore diameter, the structure with the largest value of K/D_{me} is chosen.

Our aim was to investigate the kinetics of capillary absorption by fibrous wicks with different structures and compare the results with the preliminary conclusions concerning optimum structures. All of the nine tested specimens were made in the shape of plates with a length of 500 mm, a width of 45 mm, and a

Translated from *Inzhenerno-Fizicheskii Zhurnal*, Vol. 27, No. 6, pp. 1009-1014, December, 1974.
Original article submitted January 9, 1974.

©1976 Plenum Publishing Corporation, 227 West 17th Street, New York, N.Y. 10011. No part of this publication may be reproduced, stored in a retrieval system, or transmitted, in any form or by any means, electronic, mechanical, photocopying, microfilming, recording or otherwise, without written permission of the publisher. A copy of this article is available from the publisher for \$15.00.

TABLE 1. Results of Investigation of the Structure, Permeability, and Capillary Equilibrium Height of Fibrous Wicks

$\frac{l_f}{d_f}$	$\Pi, \%$	$K \cdot 10^{11}, m^2$	$D_{me} \cdot 10^6, m$ (with respect to viscous friction)	$H \cdot 10^3, m$ (oxidized surface)		$D'_{me} \cdot 10^6, m$ (with respect to rise height)	
				water	acetone	water	acetone
45	61,2	5,6	60,0	>480	220	<62,0	55,5
	70,0	14,6	81,0	420	165	71,0	74,0
	79,2	35,5	107,0	290	120	102,5	102,0
75	70,0	7,3	60,0	>480	210	<62,0	58,0
	79,4	18,8	83,0	355	145	83,5	84,5
	88,5	45,2	108,5	180	75	165,0	163,0
150	79,0	5,5	63,0	>480	210	<62,0	58,0
	90,0	25,5	93,0	270	110	110,0	111,0
	95,0	48,3	110,0	130	55	228,0	222,0

thickness of 2 mm (the structural characteristics of the wicks are given in Table 1). The specimens were fastened inside glass tubes with a length of 510 mm and an inside diameter of 87 mm. The liquid from a feed buret was supplied at the end of the porous specimens. Indicator paper strips with a width of 3 mm were securely fastened to the wick surface by means of clamps at certain distances from each other. The clamps were connected through a multipoint switch to one terminal of an ohmmeter; the other terminal was connected to the clamp in direct contact with the metallic surface of the wick. The movement of the liquid front was determined with respect to the wetting and the resistance drop of the indicator paper.

Liquid evaporation from the wick surface was reduced to a minimum. This was achieved by hermetic sealing of the glass tube and by saturating the space around the wick with vapor of the operating liquid for a period of 1-2 h before starting an experiment. The design of the device made it possible to switch the position of the specimen from the horizontal to the vertical. In testing vertically positioned specimens, we also recorded the maximum height of capillary rise; each experiment was performed over a period of 1 to 3 days in order to ensure this.

Distilled water and acetone at $t = 20 \pm 2^\circ C$ were used as the operating liquids.

All specimens were oxidized at $t = 300^\circ C$ in order to improve the wetting of the porous structure. The movement of the impregnation front along the wick was also observed visually on oxidized specimens.

As a result of processing the experimental data, we determined the distributions of the impregnation front velocity along the wicks by means of graphic differentiation of the absorption kinetics curves.

According to the earlier experiments, the capillary pump parameter K/D_{me} , which characterizes the transport capacity of the wick in the horizontal position, increases with the porosity and the diameter of initial fibers. However, the maximum attainable porosity of the material diminishes with an increase in the fiber diameter. The maximum porosities Π_m of structures with the ratios $l_f/d_f = 150, 75, 45$ lie in the ranges 93-97%, 88-93%, 80-85%, respectively. Since the possibility of improving the capillary pump parameter is limited by the maximum porosity of each type of material, the maximum values of K/D_{me} were achieved in the previous experiments for a structure with $l_f/d_f = 75$ ($\Pi_m = 93.3\%$). Lower values of K/D_{me} were obtained for structures with a smaller ($l_f/d_f = 150$; $\Pi_m = 94.6\%$) and a larger ($l_f/d_f = 45$; $\Pi_m = 85\%$) fiber diameter.

The horizontal impregnation rate curves for specimens of three types of structure with maximum porosity are given in Fig. 1. The specimen with $l_f/d_f = 75$ and $\Pi = 88.5\%$ had the greatest transport capacity. The kinetics of horizontal absorption remained virtually unchanged after switching from one operating liquid to another. This is explained by the almost equal values of the liquid parameter σ/μ for water and acetone, which characterize the ratio of capillary forces to viscosity forces and determine the horizontal impregnation rate.

Figure 2 shows the curves for permeability factor versus mean pore diameter, obtained from the results of the preliminary investigations. Analysis of the curves shows that for any fixed value of D_{me} , which determines the capillary pressure, the structure with $l_f/d_f = 75$ possesses the highest permeability (the lowest hydraulic resistance). The assumption that this structure is also the optimum one for operation against the force of gravity is confirmed by the velocity-distribution curves. Figures 3 and 4 show the results for specimens with three different types of structure and with almost equal mean pore diameters.

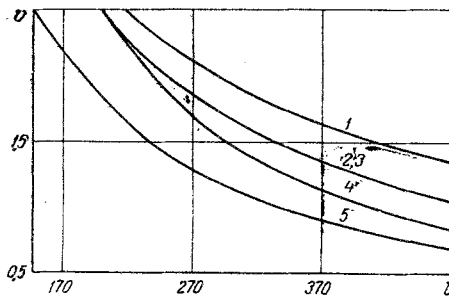


Fig. 1

Fig. 1. Velocity of the impregnation front for water and acetone at $\alpha = 0^\circ$ (v , mm/sec; l , mm): 1) $l_f/d_f = 75$ and $\Pi = 88.5\%$; 2) 45 and 79.2%; 3) 150 and 95%; 4) three layers of No. 02 gauze; 5) three layers of No. 008 gauze.

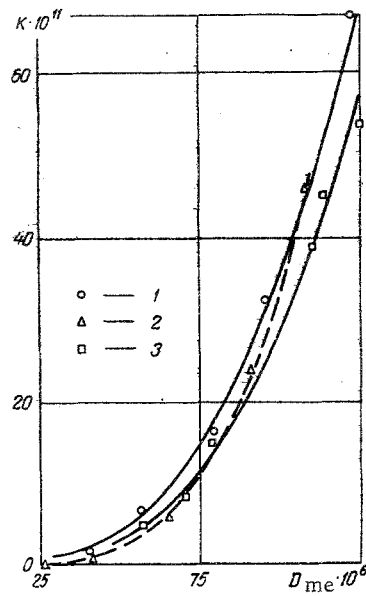


Fig. 2

Fig. 2. Permeability factor K (m^2) as a function of the mean pore diameter D_{me} (m): 1) $l_f/d_f = 75$; 2) 150; 3) 45.

The specimen with $l_f/d_f = 75$ and $\Pi = 70\%$ displayed the highest transport capacity in operation against the force of gravity. The effect of the gravitational field on the motion of liquids with different surface-tension coefficients causes sharp differences between the absorption kinetics of water and acetone.

Figure 4 shows the curve of the vertical rate of impregnation of unoxidized and oxidized specimens with acetone. A comparison between the curves demonstrates the importance of wick oxidation. If water is used as the operating liquid, wick oxidation is not only desirable, but also necessary.

The permeability factor, the mean pore diameter, and the height H of capillary equilibrium for the specimens are given in Table 1. The values of the mean pore diameter determined in previous experiments with respect to viscous friction of argon agree with the mean diameter values calculated with respect to the rise height (for $\cos \theta = 1$). Specimens with maximum porosity constituted an exception, which can be explained by the considerable effect of capillary hysteresis in their nonuniform structure. Experiments

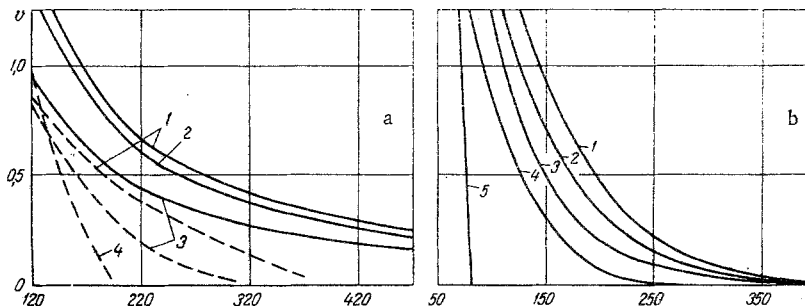


Fig. 3. Velocities of the impregnation front for water (solid curves) and acetone (dashed curves) at $\alpha = 15^\circ$ (a) and for water at $\alpha = 90^\circ$ (b): 1) $l_f/d_f = 75$ and $\Pi = 70\%$; 2) 150 and 79%; 3) 45 and 61.2%; 4) three layers of No. 0056 gauze (a) and 10 layers of ASTT S-2 glass fabric [2] (b); 5) 120-mesh gauze [5] (v , m/sec; l , mm).

TABLE 2. Comparison of Wick Characteristics

Porous structure	Material	$\Pi, \%$	$K \cdot 10^{11}, m^2$	$H \cdot 10^3, m$ (water)	$K \cdot H \cdot 10^{11}, m^3$	Literature reference
Fibrous	Nickel	86,8	4,4	>405	>1,78	[4]
Fibrous	Same	82,5	3,4	>405	>1,38	
Fibrous	"	68,9	1,5	>405	>0,61	
Fibrous	"	88,0	3,1	>400	>1,24	
Fibrous	Stainless steel	91,6	54,6	155	8,48	
Fibrous	Same	80,8	19,6	226	4,43	
Fibrous	"	82,2	116,0	135	15,70	
Latticed	Nickel	62,5	66,3	48,5	3,22	
Latticed	Same	67,9	15,2	>112	>1,70	
Latticed	"	67,6	7,7	234	1,80	
Fibrous	Copper	80,0	15,5	362	5,61	[5]
Latticed	Nickel	—	129,5	25,4	3,29	
Latticed	Stainless steel	—	34,6	79,4	2,74	
Fibrous	Stainless steel	89,0	53,1	68	3,16	[6]
Fibrous	Same	80,0	21,6	120	2,60	
Fibrous	"	58,0	3,2	257	0,82	
Fibrous	Nickel	82,0	4,9	292	1,43	
Fibrous	Same	61,0	0,5	583	0,29	
Fibrous	Copper	59,0	2,5	311	0,78	
Latticed	Stainless steel	69,0	25,4	55	1,40	
Latticed	Same	63,0	13,0	110	1,43	
Latticed	"	68,0	5,5	143	0,79	
Latticed	"	69,0	3,8	199	0,76	
Fibrous	Nickel	85,0	11,3	226	2,56	[7]
Fibrous	Same	80,0	6,6	305	2,01	
Fibrous	"	70,0	2,3	460	1,06	
Fibrous	Copper	80,0	18,6	162,5	3,02	
Latticed	Nickel	60,0	13,3	127	1,69	[7]
Latticed	Brass	72,4	640,0	—	—	[2]
Fibrous	Copper	70,0	7,3	>480	>3,5	Some of the authors' data
Fibrous	Same	79,2	35,5	290	10,30	
Fibrous	"	88,5	45,2	180	8,15	

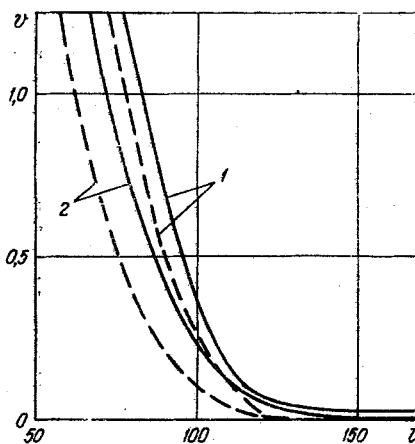


Fig. 4. Velocity of the impregnation front of acetone for oxidized (solid curves) and unoxidized (dashed curves) specimens at $\alpha = 90^\circ$ (v , mm/sec; l , mm): 1) $l_f/d_f = 75$ and $\Pi = 70\%$; 2) 45 and 61.2%.

on the lowering of the liquid in a previously soaked wick (these conditions are closer to the actual process in a heat pipe) would obviously yield larger values of the height of capillary equilibrium and, correspondingly, smaller pore diameters for specimens with maximum porosity.

Thus, the experimentally investigated kinetics of capillary absorption in metal-fiber wicks agrees with the results of the preliminary analysis of their structural and hydrodynamic characteristics.

Of the investigated three types of fibrous materials, the structure with $l_f/d_f = 75$ has the highest transport capacity. Wicks with maximum porosity should be used for heat pipes operating in the horizontal position. The porosity of a wick operating against the force of gravity should correspond to the pore diameter ensuring the required height of capillary equilibrium.

Table 2 provides a comparison between the characteristics of fibrous and latticed wicks with respect to two parameters: the capillary rise height for water and the complex KH. As in the case of K/D_{me} , the second parameter, taken separately, characterizes the horizontal transport capacity of the wick. Operation against the force of gravity is evaluated by considering these two parameters simultaneously. An analysis of Table 2 shows that fibrous wicks have considerable advantages over latticed wicks, especially in operation against the force of gravity. This conclusion is confirmed by direct comparison between the impregnation rates of various porous wicks (Figs. 1, 3a, and 3b).

The above investigations have provided a rational basis for designing heat pipes with efficient fibrous wicks.

NOTATION

l_f/d_f	is the ratio of fiber length to fiber diameter;
Π	is the wick porosity;
Π_m	is the maximum porosity;
D_{me}	is the mean pore diameter;
K	is the permeability factor;
H	is the height of capillary equilibrium;
v	is the velocity of the impregnation front;
l	is the wick length from the starting point of impregnation;
α	is the angle between the longitudinal axis of the wick and the horizontal plane;
θ	is the wetting contact angle of the wick material;
σ	is the surface-tension coefficient of the liquid;
μ	is the dynamic viscosity of the liquid.

LITERATURE CITED

1. L. L. Vasil'ev, Z. N. Kostko, and S. V. Konev, *Inzh.-Fiz. Zh.*, 23, No. 4, 606 (1972).
2. Z. N. Kostko, in: *Low-Temperature Energy and Matter Transport in a Vacuum* [in Russian], Minsk (1973), p. 132.
3. J. C. Chato and J. H. Streckert, Performance of a Wick-Limited Heat Pipe, ASME Paper, No. 69-HT-20 (1969).
4. L. S. Langston and H. R. Kunz, Liquid-Transport Properties of Some Heat-Pipe Wicking Materials, ASME Paper, No. 69-HT-17 (1969).
5. R. A. Freggens, "Experimental determination of wick properties for heat-pipe applications," Proceedings of the Fourth Intersociety Energy Conversion Engineering Conference, Washington (1969).
6. J. K. Ferrell, E. G. Alexander, and W. T. Piver, Vaporization Heat Transfer in Heat-Pipe Wick Materials, AIAA Paper, No. 256 (1972).
7. J. C. Corman and G. E. Walmet, Vaporization from Capillary Wick Structures, ASME Paper, No. HT-35 (1971).